ACS OMEGA

http://pubs.acs.org/journal/acsodf

Article

Development and Performance Evaluation of an Intelligent Sand Control Screen Based on Polyphenylene Sulfide

Yuanwei Sun,* Dexu Sun, Yizhong Zhao, Yeping Gao, Cui Li, Xiaodong Dai, Yanli Wang, and Yuanfang Cheng

Cite This: *ACS Omega* 2022, 7, 18063−18072

Read Online

ACCESS | Metrics & More | Article Recommendations

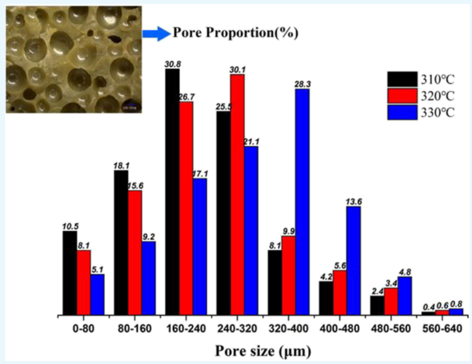

ABSTRACT: Open hole combined with a sand filter pipe is the main development mode of an unconsolidated sandstone horizontal well, which causes problems such as shaft wall collapse, sand filter pipe blockage, and even damage. At present, the polyurethane intelligent sand control screen pipe can effectively solve these problems, but its application scope is limited by the downhole temperature and material strength. Therefore, the high-strength shape memory polyphenylene sulfide (SMPPPS) was synthesized by an indoor experiment, then the shape memory performance was analyzed, and the variation law of pore size with composition and processing technology was obtained. Finally, the performance of the SMPPPS intelligent screen was evaluated. It is found that (1) with the increase of the cross-linking agent content, the melt index and melt peak temperature of SMPPPS decrease rapidly at first and then remain unchanged; the cross-linking agent content is set at 4.5 wt %. (2) The shape memory performance of SMPPPS is good, and the recovery ratio can reach 99.8% at 110 °C in 11.8 min. (3) The relationship between the pore size distribution proportion of SMPPPS and the foaming agent content, pore enhancer content, temperature, and pressure is determined through experiments; the main distribution range of pore size increases with the increase of the foaming agent content and temperature and decreases with the increase of the pore enhancer content and pressure. When the foaming agent content is 0.5 wt %, the pore enhancer concentration is 10 wt %, the molding temperature is 320 °C, the molding pressure is 10 MPa, and the main distribution range of pore size is 80−320 μm. (4) The permeability of recovery SMPPPS with a compression ratio of 300% first increases slightly and then decreases slightly with the increase of flow, with a variation range of 420.5−463 mD; the compressive strength range is 9.5−11.4 MPa; the SMPPPS has good adaptability to downhole fluid; the sand retaining accuracy is higher than that of the screen sand filter pipe, but the blockage is more serious.

1. INTRODUCTION

Unconsolidated sandstone reservoirs are the main type of reservoir developed at present, but due to loose cementation, this kind of reservoir is easy to produce sand, resulting in sand burial, sand plugging, causing damage, and even scrapping of oil and gas wells.[1−4] In recent years, the development of loose sandstone horizontal wells has mainly been based on open holes combined with sand filter pipes for sand control, which can reduce the construction risk of high-pressure operations and save operation costs. However, three major problems have been exposed: the collapse of the open hole wall of horizontal wells leads to the deformation and damage of the sand filter pipe; the sand filter pipe has poor erosion resistance and is easily blocked; the bottom reverse extrusion filling sand control process is not perfect, resulting in the deformation and damage of the screen tube.[5−11] In view of the abovementioned problems, the shape memory polymer (SMP) material is used to develop an intelligent screen with shape memory to completely fill the gap between the bottom hole space and the casing to achieve efficient sand control, which provides a new improved method for the sand control technology of open-hole horizontal wells.[12−14]

In the field of the petroleum industry, SMP materials are gradually applied to oil well sand control, drilling fluid plugging, sealing well sections, and other aspects, which have produced remarkable benefits.[15−20] The application of SMP materials in drilling fluid plugging was studied, which greatly improved the operation efficiency.[21−24] The SMP materials were applied to the field of expandable cement, improving the cement formula suitable for different downhole temperatures and improving the cementing effect.[25,26] In recent years, shape

Received: March 15, 2022
Accepted: May 4, 2022
Published: May 18, 2022

https://doi.org/10.1021/acsomega.2c01550
ACS Omega 2022, 7, 18063−18072

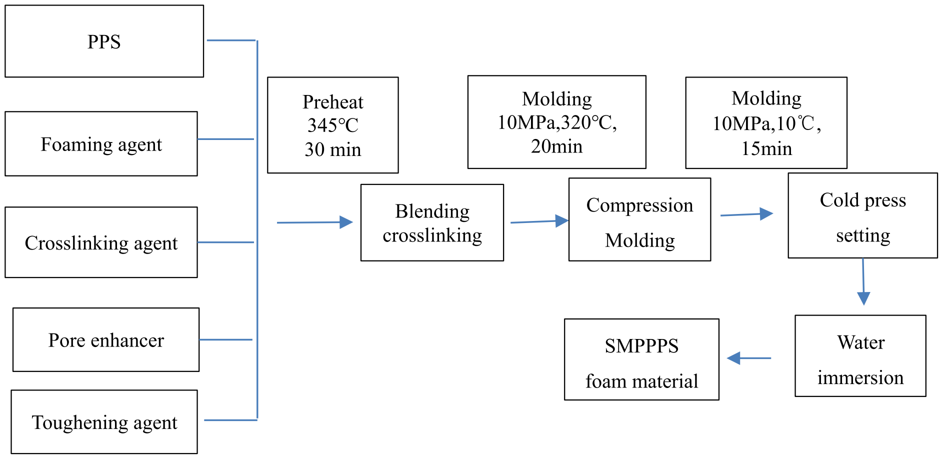

Figure 1. Flow chart of cross-linked PPS foam preparation.

memory materials represented by polyurethane have been deeply studied and widely used. Glycerol as a cross-linking agent was used and the chemical cross-linking point on the basis of the physical cross-linking point was introduced to synthesize low degree cross-linked polyurethane, whose Young's modulus was greatly improved at low temperature and its ability to fix shape was greatly enhanced.[27] A polyurethane material with good thermodynamic properties and shape memory properties was developed with a compression ratio of 400% and a shape recovery temperature of about 60 °C.[14] A filled polycaprolactone-based shape memory polyurethane foam was developed with better deformation, excellent memory, and filtration performance.[28,29] It has the potential to be a sand control screen material, and the processing technology is simpler. However, in general, shape memory polyurethane materials face the problems of a low recovery temperature range and compressive strength, which limit their application range.

Polyphenylene sulfide (PPS) is a new thermoplastic material with vigorous development. The cross-linked PPS-molded products have good reproducibility, excellent chemical resistance, good mechanical properties, excellent fatigue resistance, and creep resistance,[30,31] which makes them a good choice of a sand control screen material. Therefore, in view of the shortcomings of open-hole sand filter tubes and polyurethane intelligent sand control screen tubes in loose sandstone sand control technology, a new type of high-strength shape memory PPS (SMPPPS) intelligent sand control screen tubes is being developed, comprehensively considering the characteristics of the oil well formation temperature, downhole working environment, and required material properties. In this paper, the shape memory performance of SMPPPS is analyzed, the variation law of pore size with composition and processing technology is explored, and the sand control performance is evaluated, which has important theoretical and practical guiding significance for improving the adaptability of sand control technology in loose sandstone reservoirs and prolonging the effective period of sand control. It can provide strong theoretical and technical support for promoting the progress of sand control technology in loose sandstone oilfields.

2. PREPARATION AND PERFORMANCE ANALYSIS

2.1. SMPPPS Intelligent Material Raw Materials and Processing Equipment. The experimental materials include the following: resin PPS; cross-linking agent anthraquinone; cross-linking agent tetrachlorobenzoquinone; foaming agent melamine; pore enhancer NaCl; toughening agent Fluororubber (FKM); toughening agent Nitrile Butadiene Rubber (NBR); deionized water; sewage, salinity 10 895.42 mg/L, $CaCl_2$ type, ion composition (unit: mg/L): Cl^- 5865.42, K^+ + Na^+ 3862.13, HCO_3^- 487.86, Ca^{2+} 384.26, and Mg^{2+} 46.68, SO_4^{2-} 42.36; clean water, ion composition (unit: mg/L): Cl^- 245, SO_4^{2-} 245, Ca^{2+} 0.98, and Mg^{2+} 0.98; brine, distilled water 995.42 g/L, sodium sulfate 0.130 g/L, sodium chloride 4.642 g/L, anhydrous calcium chloride 0.218 g/L, magnesium chloride hexahydrate 0.228 g/L, and sodium bicarbonate 0.548 g/L; Lr520 kerosene; sodium hydroxide 10%; and acid 10%.

The experimental equipment includes the following: VFP-F500 planetary ball mill; CLF-04 crusher; H-2050R centrifuge; TAW-3000 servo control equipment for rock mechanics; BWS constant temperature water tank and water bath pot; Q800 dynamic thermomechanical performance analyzer; DW-3 digital display electric agitator; DSC-1 STAR differential scanning calorimeter; and VEGA-3 SBH scanning electron microscope.

2.2. Development Scheme and Effect Analysis of SMPPPS Intelligent Material. The preparation process of the SMPPPS intelligent material is as follows. (1) PPS resin, toughening agent fluororubber, and pore-increasing agent NaCl were crushed using a pulverizer, and PPS powder was vacuum dehydrated for 1.5 h to make its moisture content less than 0.1%, so as to obtain pure PPS powder. (2) PPS and toughening agent fluororubber were ball milled, in which the content of fluororubber was 15 wt %, the rotating speed of the planetary ball mill was 300 rpm, and the PPS mixture was evenly mixed after ball milling for 10 min. (3) The PPS mixture, cross-linking agent tetrachlorobenzoquinone (concentration: 0−7.5 wt %), foaming agent melamine (concentration: 0−1.0 wt %), and pore enhancer NaCl (concentration: 0−15 wt %) were preheated at 345 °C for 30 min. (4) According to the proportion set in the experiment, different concentrations of the cross-linking agent, foaming agent, and pore-increasing agent were added to the PPS mixture in turn, and stirred at high speed for 5 min to make it fully mixed and uniform. (5) Quickly pour the PPS mixture after stirring into

https://doi.org/10.1021/acsomega.2c01550
ACS Omega 2022, 7, 18063−18072

the mold pre-coated with the release agent, and conduct foaming under molding pressure (5−15 MPa) and molding temperature (310−330 °C) for 20 min. (6) Under the molding pressure, quickly reduce the molding temperature to below 10 °C, then cold press for 15 min and demold to obtain the compressed SMPPPS intelligent memory material. The process is shown in Figure 1.

Figure 2 shows the shape memory properties of SMPPPS prepared by the cross-linking method. When the temperature

Figure 2. Shape memory performance of cross-linked PPS at different temperatures.

reaches the glass transition temperature of 110 °C, the shape is basically completely restored, indicating that the shape memory performance is good.

2.3. SMPPPS Performance Analysis. *2.3.1. Melting Index Law Analysis.* The melt index of pure PPS at 290 °C and the melt index of PPS at 320 °C with different dosages of the cross-linking agent (0.0, 1.5, 3.0, 4.5, 6.0, and 7.5 wt %) were tested, respectively, as shown in Figure 3. The melt index

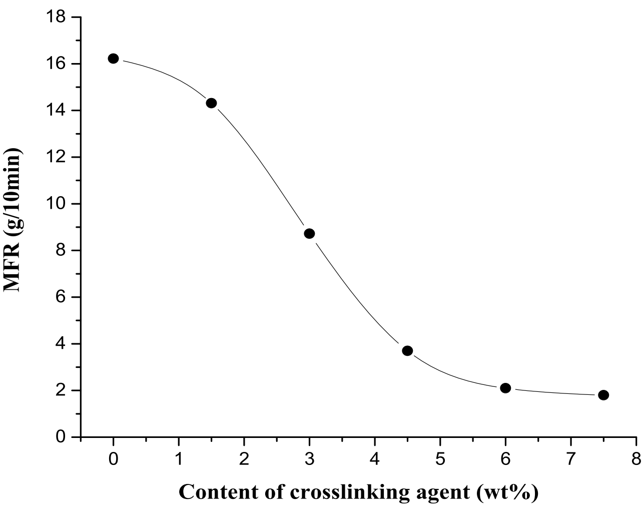

Figure 3. Melting index of SMPPPS with different dosages of the cross-linking agent.

of pure PPS is 45.62 g/10 min at 290 °C and 16.22 g/10 min at 320 °C, indicating that the melt index of PPS decreases significantly and the fluidity decreases after high-temperature heat treatment. With the increase of the cross-linking agent content, the melt index of PPS first decreases rapidly. When the cross-linking agent content exceeds 4.5 wt %, the downward trend slows down, indicating that the increase of the cross-linking agent content will enhance the oxidative cross-linking reaction of PPS, reduce the fluidity, and improve the processing performance. Therefore, the cross-linking agent content can be 4.5 wt %.

2.3.2. Differential Scanning Calorimetry. The prepared samples were tested by differential scanning calorimetry (DSC) using the secondary heating curve method, and the melting peak temperatures under different cross-linking agent contents (0, 1.5, 3.0, 4.5, 6.0, and 7.5 wt %) were obtained, as shown in Figure 4. With the increase of the cross-linking agent

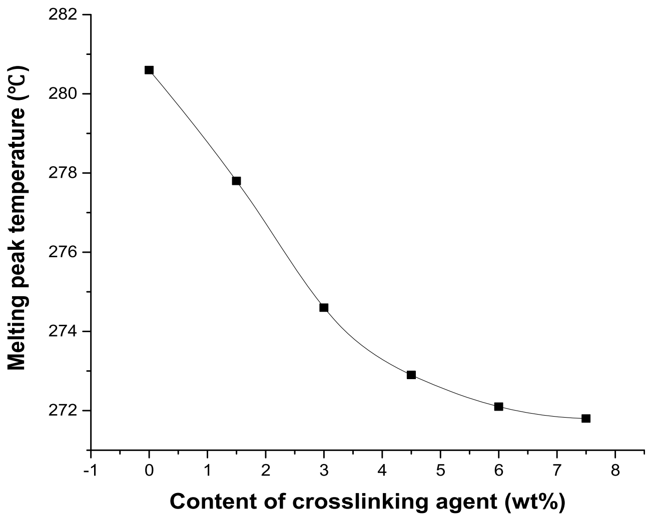

Figure 4. DSC curves of SMPPPS with different cross-linking agent.

content, the melting peak temperature of SMPPPS decreases, but the decreasing range slows down. Mainly because with the increase of the cross-linking agent content, the crystallinity decreases and the amorphous area of cross-linking increases, which is conducive to shape fixation in the process of shape memory. Finally, the content of the cross-linking agent is set at 4.5 wt %.

2.3.3. Dynamic Thermomechanical Analysis. The shape memory properties of SMPPPS were quantitatively characterized by thermomechanical cycle tests. The sample is stretched to 50% deformation at a rate of 10 mm/min at 110 °C, kept for 5 min, then cooled to 10 °C at a cooling rate of 10 °C/min and fixed as a temporary shape for 5 min, and then heated to 110 °C at a heating rate of 10 °C/min to stimulate the sample to return to its original shape, so as to obtain the stress, strain, and temperature changes during a complete cycle, as shown in Figure 5.

The deformed SMPPPS slowly recovers its shape with the increase in temperature. When the temperature reaches 70.1 °C, it begins to accelerate the recovery. When the temperature reaches 100 °C, the shape recovers to about 90%, and when the temperature reaches 110 °C, the recovery rate reaches 99.8%, which means the shape memory performance is good. Figure 6 shows the change of the SMPPPS shape recovery ratio with time, and Figure 7 shows the shape recovery rate. SMPPPS can recover to about 90% in 9.1 min and 99.8% in 11.8 min. The maximum recovery speed occurs in 8 min, which is 26.05%/min.

3. ANALYSIS ON THE INFLUENCING FACTORS OF SMPPPS PORE STRUCTURE

3.1. Effect of the Foaming Agent on Pore Structure. Figure 8 shows the pore morphology and structural characteristics of SMPPPS foam with the foaming agent content of 0.25, 0.50, and 1.0 wt %. The foam material is made of pore holes,

https://doi.org/10.1021/acsomega.2c01550
ACS Omega 2022, 7, 18063−18072

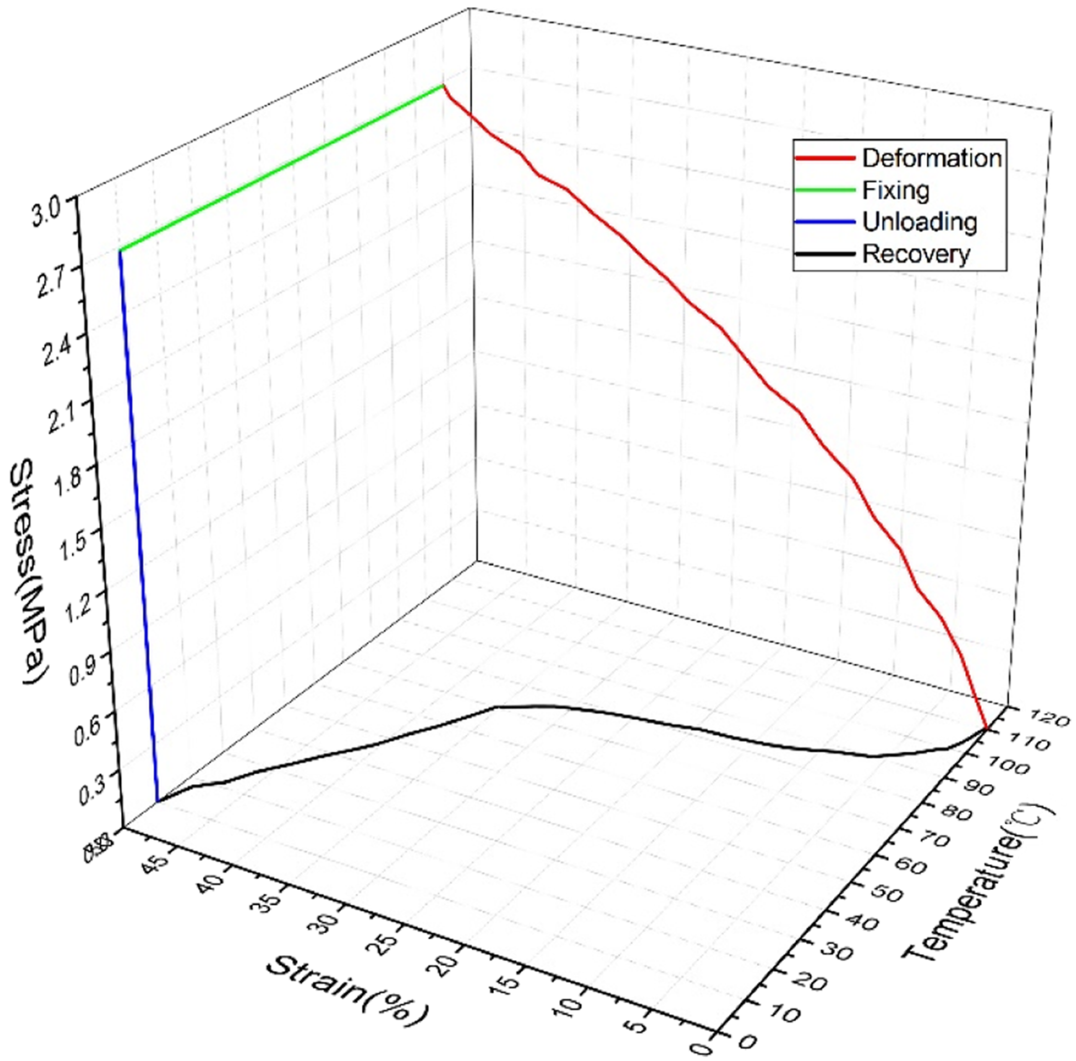

Figure 5. Thermomechanical circulation of SMPPPS.

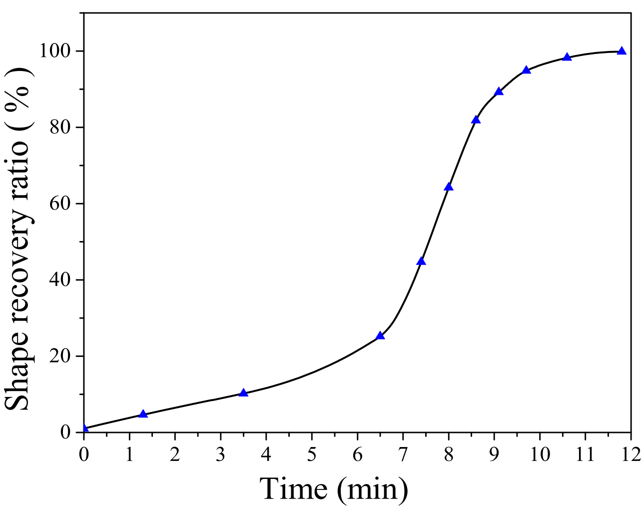

Figure 6. Shape recovery ratio of SMPPPS with time.

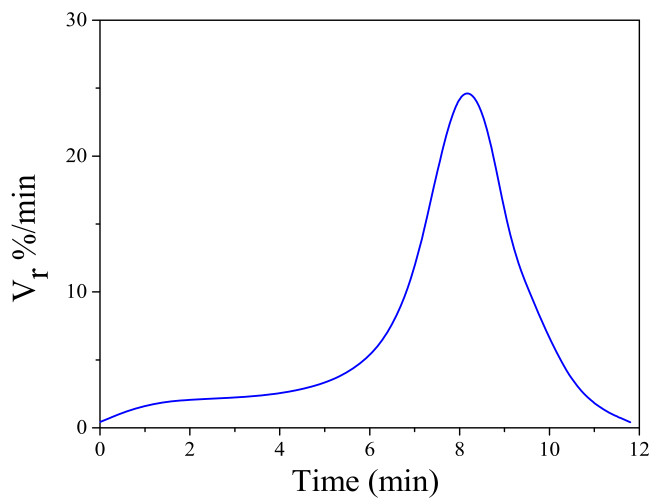

Figure 7. Shape recovery rate of SMPPPS with time.

and there are some perforated holes on the wall. The pore size is related to the foaming agent content. The more the foaming agent content, the larger the pore size; due to the addition of foaming agents in the system, the strength of the pore wall is reduced. In the foaming process, the pore wall is broken by gas, resulting in a broken wall shape and cavity.

In order to analyze the influence of foaming agent content on the flow channel of SMPPPS material, the pore size and proportion were measured, as shown in Figure 9. (1) SMPPPS

https://doi.org/10.1021/acsomega.2c01550
ACS Omega 2022, 7, 18063−18072

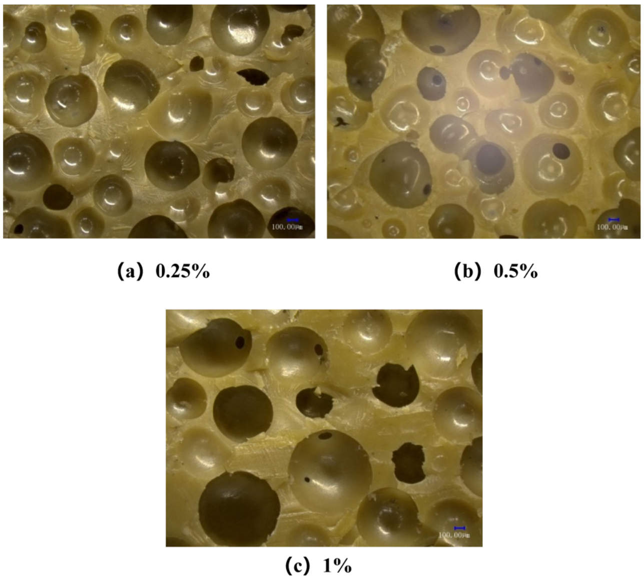

Figure 8. Pore structure of SMPPPS by different foaming agent contents.

has a large distribution range of pore size, but with the increase of pore size, its proportion first increases and then decreases, and there is a main distribution range of pore size. (2) The pore size is significantly affected by the foaming agent content. With the increase of the foaming agent content, the pore size of SMPPPS shows an increasing trend. When the foaming agent content is 0.25%, the main distribution range of pore size is 80−320 μm. The proportion reached 70.90%; when the foaming agent content is 0.5%, the main distribution range of pore size is 160−400 μm. The proportion reached 72.30%; when the foaming agent content is 1.0%, the main distribution range of pore size is 180−480 μm. The proportion reached 76.08%. (3) The pore size is related to the foaming agent content. The sand control effect depends on the combination of the sand particle size and pore size. Therefore, the foaming agent content should be determined according to the sand particle size.

3.2. Effect of the Pore Enhancer on Pore Structure. In order to increase the water permeability of SMPPPS, NaCl with a decomposition temperature of 800 °C was selected as the pore enhancer. During the experiment, the content of the foaming agent was 0.5 wt %, and the pore enhancer concentrations were 5, 10, and 15 wt %, respectively. The cross section was observed using a scanning electron microscope, and the pore size and proportion were statistically analyzed, as shown in Figure 10. (1) With the increase of the NaCl content, the pore size decreases and there is obvious shrinkage, but the number and uniformity of pores increase; the reason is that after NaCl dissolves, the strength of the foam hole wall decreases, the hole wall becomes soft, and the cavity shrinks during the drying process. (2) When the NaCl content is 5 wt %, the main distribution range of pore size is 160−400 μm and the proportion reached 71.94%; when the NaCl content is 10 wt %, the main distribution range of pore size is 80−320 μm and the proportion reached 73.64%; when the NaCl content is 15 wt %, the main distribution range of pore size is 80−320 μm and the proportion reached 76.00%.

The addition of NaCl significantly increases the pore opening rate of PPS, but too much dosage will make the molding of PPS more difficult and reduce the mechanical properties of PPS. Therefore, after comprehensive consideration, the content of pore enhancer NaCl should not exceed 15%.

3.3. Effect of Molding Foaming Temperature. During the experiment, the foaming agent content is 0.5 wt %, the pore enhancer concentration is 10%, and the molding temperatures are 310, 320, and 330 °C, respectively. The pore size distribution of SMPPPS foam with different molding temperatures is shown in Figure 11.

From Figure 11, (1) with the increase of the molding foaming temperature, the main distribution range of pore size increases because the increase in temperature makes the foaming agent more thoroughly decomposed and the foaming effect better. (2) When the molding temperature is 310 °C, the main distribution range of pore size is 80−320 μm; when the molding temperature is 320 °C, the main distribution range of pore size is 80−320 μm; when the molding temperature is 330 °C, the main distribution range of pore size is 160−400 μm.

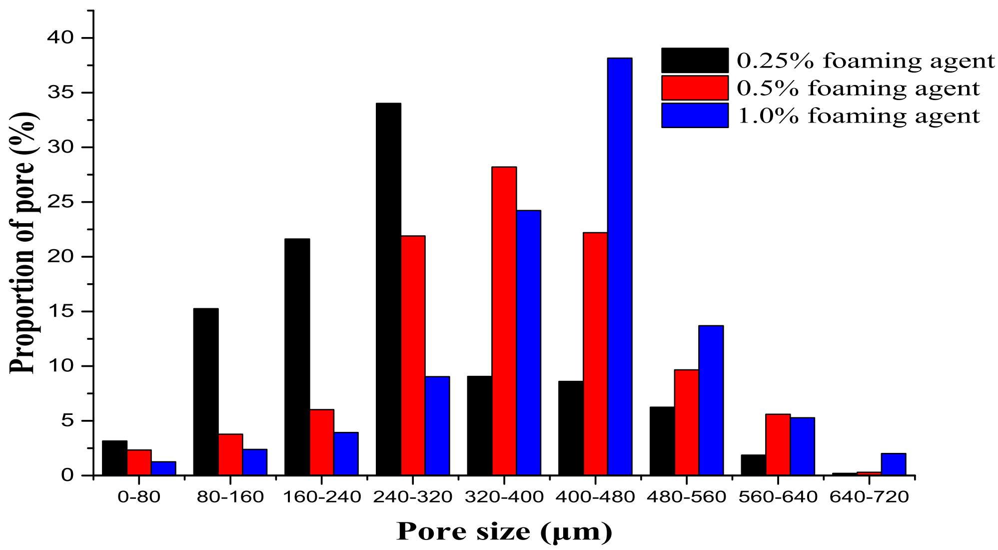

Figure 9. SMPPPS pore size pattern with different foaming agent contents.

https://doi.org/10.1021/acsomega.2c01550
ACS Omega 2022, 7, 18063−18072

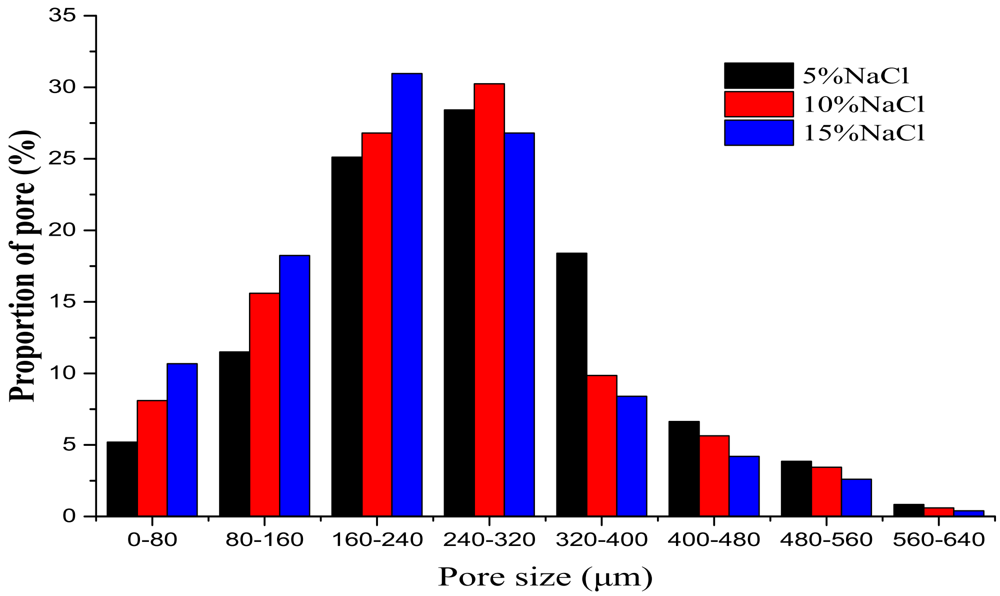

Figure 10. Pore structure of SMPPPS with different NaCl contents.

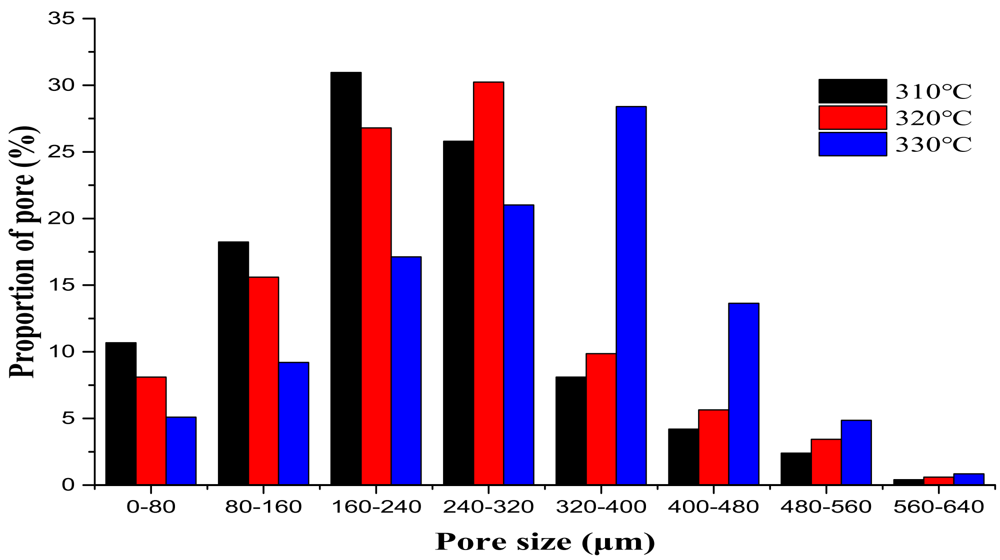

Figure 11. Pore structure of SMPPPS by different molding foaming temperatures.

However, it should be noted that too high a temperature will also cause serious coloring and adverse effects.

3.4. Effect of Molding Foaming Pressure. During the experiment, the foaming agent content is 0.5 wt %, the pore enhancer concentration is 10%, the molding temperature is 320 °C, and the molding temperatures are 310, 320, and 330 °C, respectively. The pore size of SMPPPS foams prepared by different molding pressures is shown in Figure 12.

From Figure 12, (1) with the molding pressure increasing, the pore size will decrease accordingly, and the pore will be more dense and uniform, leading to the increase of SMPPPS density. However, when the molding pressure reaches 15 MPa, a small amount of large holes will appear in the material, which is caused by the rupture of pores in the resin and the accumulation of gas to form larger pores. (2) When the molding pressure is 5 MPa, the main distribution range of pore size is 160−480 μm; when the molding pressure is 10 MPa, the main distribution range of pore size is 80−320 μm; when the molding pressure is 15 MPa, the main distribution range of pore size is 0−240 μm.

4. PERFORMANCE EVALUATION OF SMPPPS INTELLIGENT SAND CONTROL SCREEN

The performance evaluation of the SMPPPS screen tube is studied by using the physical model device of the screen tube with its actual size. Figure 13 shows the SMPPPS screen structure. Before going down the well, the length of the screen tube is 1 m, the outer diameter is 196 mm, the inner diameter is 177.8 mm, and the thickness of SMPPPS is 9.1 mm. After going down the well, the screen tube has an outer diameter of 240 mm, an inner diameter of 177.8 mm, and an SMPPPS thickness of 31.1 mm.

4.1. Permeability Evaluation. SMPPPS samples were prepared at 320 °C, 10 MPa, 0.5 wt % foaming agent, and 10% pore enhancer. The core displacement experiment was carried out after the recovery of SMPPPS with a compression ratio of

https://doi.org/10.1021/acsomega.2c01550
ACS Omega 2022, 7, 18063−18072

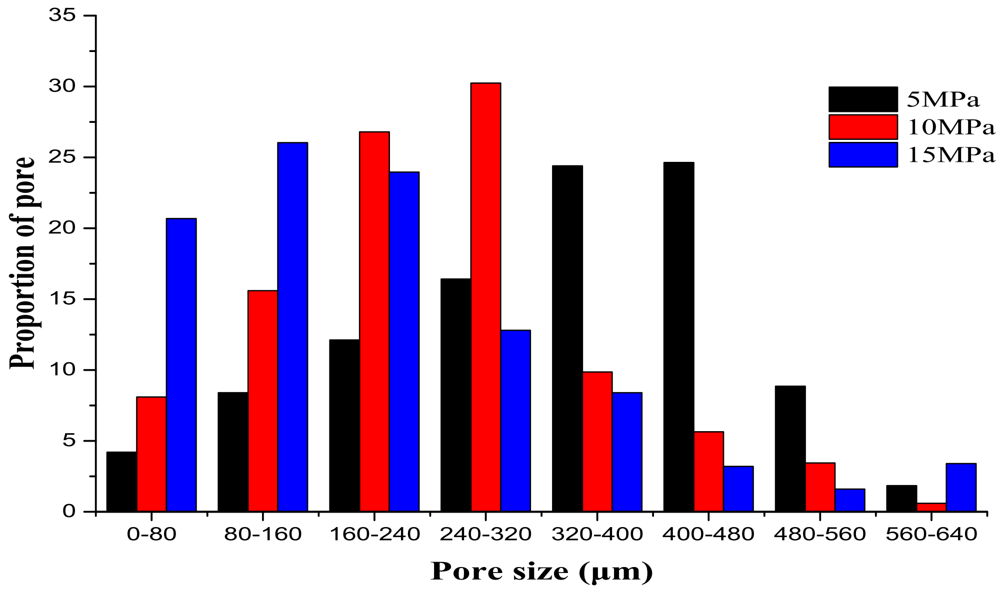

Figure 12. Pore size of SMPPPS by different molding foaming pressures.

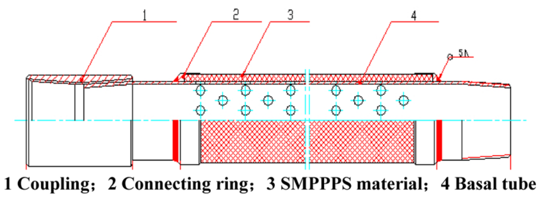

Figure 13. Machining schematic diagram of 5 1/2 in the SMPPPS screen tube sample.

300%. Here, the compression ratio can be determined by (sample volume after compression − sample volume before compression)/sample volume before compression. The displacement flow varied from 4.0 to 18.4 mL/min, and the annular pressure was 4 MPa. Figure 14 shows the permeability variation curve. With the increase of flow, the permeability of SMPPPS does not have a constant value but first increases slightly and then decreases slightly. The variation range is

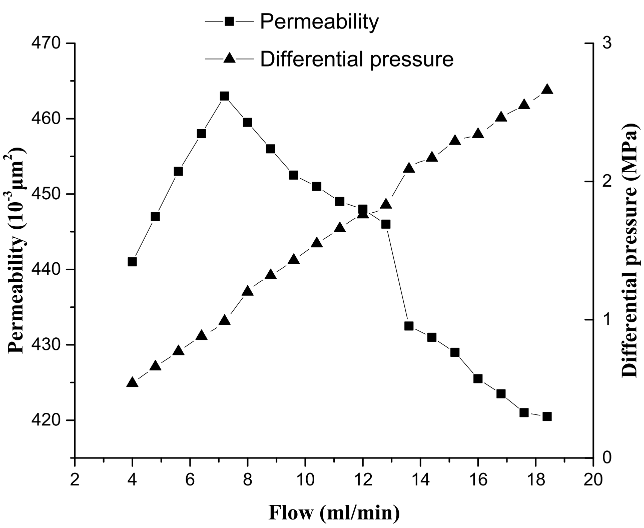

Figure 14. Permeability curve of recovery SMP samples with a compression ratio of 300%.

420.5−463 mD, and the variation range is small. When the flow rate increases, the pressure difference of SMPPPS increases nonlinearly, and there is a phased small jump in the middle, which corresponds to a small decline in material permeability. The reason is that when the flow rate exceeds 13.6 mL/min, the pressure difference at both ends of the material increases, resulting in a slight deformation of the material, and then the pressure difference and permeability change accordingly.

4.2. Compressive Strength Evaluation. The compressive strength of SMPPPS samples was tested by rock mechanics servo control equipment. Because there are pores in the sample, the test goes through the stage of elastic deformation−plastic deformation−densification, so the loading rate in the test should not be too large, which is 1 mm/min. The compressive strength of the sample increases with the increase of strain, but the excessive deformation will inevitably reduce its permeability, so the strength when the strain is 15% is selected as its compressive strength after comprehensive consideration. The results are shown in Figure 15.

From Figure 15, the middle part of the SMPPPS sample is prominent during compression. It shows that the SMPPPS is denser, the foam wall is thicker, and the compressive strength is higher. The compressive strength range of SMPPPS tested by the compressive test is 9.5−11.4 MPa.

4.3. Downhole Fluid Adaptability Evaluation. Considering the downhole environment, the SMPPPS screen tube is immersed in different media at 110 °C to evaluate its downhole fluid adaptability, as shown in Table 1. The acid is a mixture of 12% hydrochloric acid and 3% hydrofluoric acid.

Table 1 shows that, when the SMPPPS sample is immersed in the abovementioned fluid for 48 h, the sample quality increases greatly; however, it increases slowly when the soaking time is 240 h, indicating that the material has a strong ability to adsorb fluid at the beginning. After drying, the sample quality increases by different ranges compared with that before soaking, among which the increase is the most after soaking in sewage and kerosene but less than 10%. After acid−base soaking, the sample quality increases slightly, indicating that the sample basically does not react with acid−base and there is

https://doi.org/10.1021/acsomega.2c01550
ACS Omega 2022, 7, 18063−18072

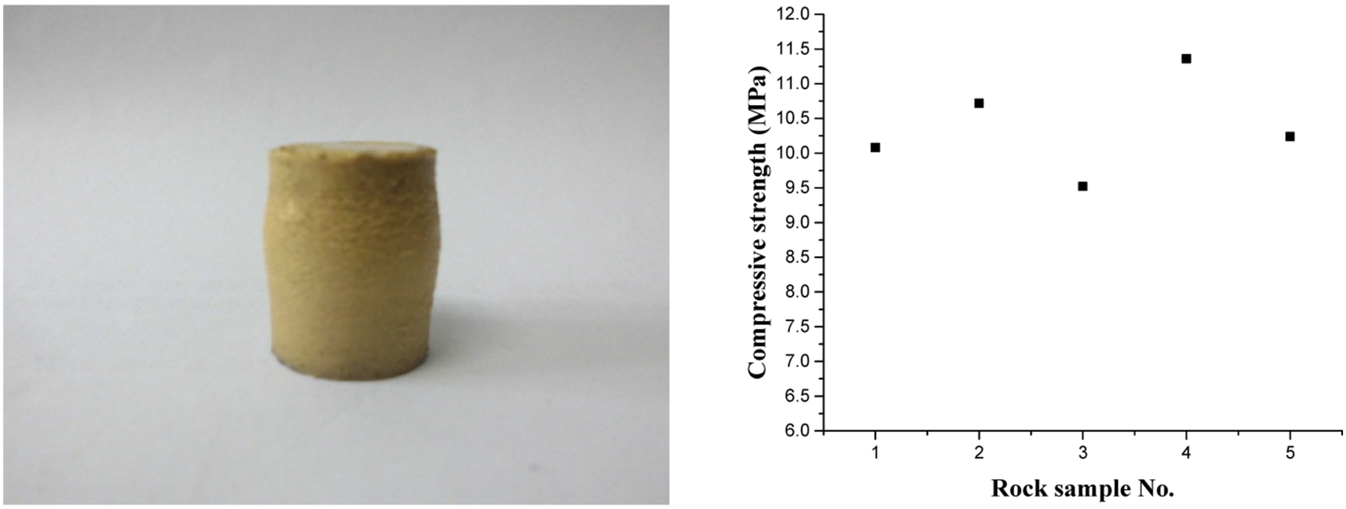

Figure 15. Compressive strength test deformed sample and test results.

Table 1. Downhole Fluid Adaptability Evaluation of SMPPPS

soaking medium	SMPPPS sample mass change ratio			
	soak for 0 h (%)	soak for 48 h (%)	soak for 240 h (%)	after drying (%)
clean water	0	40.74	52.78	1.27
brine	0	42.59	65.78	4.97
sewage	0	34.39	36.13	9.76
kerosene	0	21.67	29.81	8.24
10% acid	0	63.13	71.79	2.87
10% alkali	0	45.91	55.68	1.66

also no acid−base attached to the sample. Therefore, SMPPPS has good adaptability to the downhole fluid.

4.4. Evaluation of SMPPPS Sand Control Performance. *4.4.1. Blockage Evaluation of SMPPPS Sand Screen.* Based on the sand particle size distribution of the main oil formation of Gudong oilfield, the sand for the simulation test is configured. The characteristic value of formation sand is D_{40} and the particle size parameter is 218.7 μm. The amount of formation sand is 171 L, the mud content of formation sand is 10%, the nonuniformity coefficient is 4.08, and the displacement medium is clean water. The 5 1/2 in. screen sand filter tube and SMPPPS screen tube samples are used for experiments, respectively, and the results are shown in Figure 16. Under the experimental conditions, the flow rate increases from 380 to 1475 L/h, and the corresponding liquid production is 0.12 to 36.40 m^3/day, which is consistent with the production of most oil wells in the Gudong oilfield.

As shown in Figure 16, with the increase in flow, the pressure difference of the two kinds of screen tubes also increases. However, the pressure difference of the screen sand filter pipe is 0.05−0.17 MPa, and the pressure difference of the SMPPPS screen pipe sample is slightly larger, at 0.12−0.44 MPa. May be it is caused by the deformation and blockage of the SMPPPS screen pipe, but it is within the acceptable range.

4.4.2. Sand Retaining Accuracy Evaluation of SMPPPS Sand Control Screen. The sand content and the maximum sand particle size are used as the evaluation indexes of the sand control performance of screen tubes. The sand content and maximum particle size of the SMPPPS screen sample are shown in Figure 17.

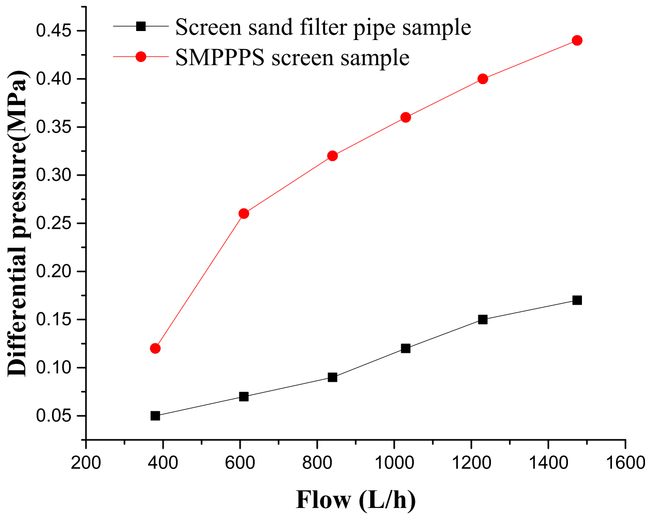

Figure 16. Comparison of pressure difference between the SMPPPS screen and the screen sand filter pipe.

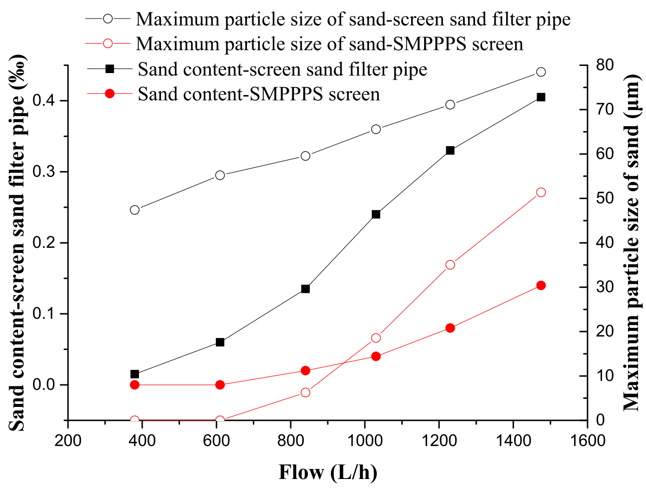

Figure 17. Curves of sand content and maximum particle size with flow.

From Figure 17, the flow rate increases from 380 to 1475 L/h, the sand content obtained by the screen sand filter screen increases from 0.02 to 0.41‰, and the maximum sand particle size increases from 47.40 μm to 78.48 μm. In contrast, the SMPPPS sample has basically no sand production when the flow is small (840 L/h). Subsequently, with the increase of flow, sand particles begin to appear, and the sand production is 0.14‰, which is about 1/3 of that of the ordinary screen sand filter screen tube. The maximum sand particle size is smaller than that of the screen sand filter tube. It means that the sand retaining accuracy of the screen tube test sample is high and meets the sand control requirements of downhole tubing. However, it also shows that the blockage of SMPPPS is more serious than that of the sand filter pipe.

5. DISCUSSIONS

Thermotropic shape memory materials represented by polyurethane have developed rapidly in recent years, which are also widely used in the field of petroleum engineering. It is hoped that this technology can solve the problems of incomplete contact between the outer diameter of the pipe and the well wall, collapse of the well wall, and damage of the sand filter pipe in horizontal open hole completion and sand filter pipe sand control, so as to improve the efficiency of sand control. Shape memory polyurethane screen tube has excellent shape memory function, which solves the abovementioned problems to a certain extent, but there are several problems. (1) The shape recovery temperature is low, the recovery starts at 43.1 °C, the recovery ratio reaches 90% at 60 °C, and there is a risk of being stuck when running underground.[14] (2) The compressive strength is low, which is 1−3 MPa. It is easy to deform under external force, resulting in large changes in permeability. (3) The pore size is small, about 150 μm, and the permeability is 200 mD, making it easy to be blocked by sand during the sand control.[14,32]

Therefore, in view of the problems of shape memory polyurethane materials, this paper attempts to develop a new SMPPPS material, explore its thermodynamic properties and shape memory properties, and evaluate its downhole sand control performance. Through the research, it was found that it has good thermodynamic performance and a high recovery temperature. The recovery ratio reaches about 90% at 100 °C, which is suitable for the increase of well depth. The compressive strength range is 9.5−11.4 MPa, and the underground deformation degree is small. Under the action of different factors, the change range of pore size is large, the permeability reaches 450 mD, and the fluidity is better. These characteristics make up for the shortcomings of the shape memory polyurethane screen pipe to a certain extent, leading to a better sand control effect and a good field application effect.

However, through the research, there are also several problems. The SMPPPS sample faces a blockage problem, which is slightly less than the shape memory polyurethane screen pipe but more serious than the sand filter pipe. The SMPPPS material is brittle, but the toughness is not enough, and its pore uniformity is slightly poor. It is necessary to further refine it to improve composition and processing technology. Finally, the overall application effect also needs to be tested on site.

6. CONCLUSIONS

(1) High-strength SMPPPS was synthesized, with the thermodynamic properties and shape memory properties analyzed. It was found that with the increase of the cross-linking agent content, the melting index and melting peak temperature of SMPPPS decreased rapidly at first and then remained basically unchanged. The cross-linking agent content was selected as 4.5 wt %. The shape memory function of SMPPPS was good, whose recovery ratio can reach 99.8% at 110 °C in 11.8 min.

(2) Carry out experiments to explore the relationship between the pore size distribution proportion of SMPPPS and the foaming agent content, pore enhancer, temperature, and pressure. It is found that the main distribution range of pore size increases with the increase of the foaming agent content and temperature, and decreases with the increase of the pore enhancer content and pressure. The pore size range can be determined by sand particle size, and then the material influence variable parameters can be deduced. When the foaming agent content is 0.5 wt %, the pore enhancer concentration is 10%, the molding temperature is 320 °C, the molding pressure is 10 MPa, and the main distribution range of pore size is 80−320 μm.

(3) The SMPPPS intelligent screen tube is designed and prepared, and the performance is evaluated. It is found that the permeability of SMPPPS with a compression ratio of 300% is not a constant value after recovery but has a variation range of 420.5−463 mD. The compressive strength range of SMPPPS is about 9.5−11.4 MPa. The SMPPPS has good adaptability to downhole fluids (brine, kerosene, acid, alkali, etc.), high sand retaining accuracy, and low sand production, which is about 1/3 of that of the ordinary screen, but the blockage is more serious.

■ AUTHOR INFORMATION

Corresponding Author

Yuanwei Sun − *College of Petroleum Engineering, Shandong Institute of Petroleum and Chemical Technology, Dongying 257061, China; School of Petroleum Engineering, China University of Petroleum (East China), Qingdao 266580, China;* orcid.org/0000-0002-4159-3346; Email: 2015004@slcupc.edu.cn

Authors

Dexu Sun − *Binnan Oil Production Plant of Shengli Oilfield Branch of Sinopec, Binzhou 251700, China*

Yizhong Zhao − *Shengli Oilfield Petroleum Development Center Company Limited, Dongying 257000, China*

Yeping Gao − *School of Petroleum and Chemical Engineering, Dongying Vocational College, Dongying 257091, China*

Cui Li − *College of Petroleum Engineering, Shandong Institute of Petroleum and Chemical Technology, Dongying 257061, China*

Xiaodong Dai − *College of Petroleum Engineering, Shandong Institute of Petroleum and Chemical Technology, Dongying 257061, China*

Yanli Wang − *College of Petroleum Engineering, Shandong Institute of Petroleum and Chemical Technology, Dongying 257061, China*

Yuanfang Cheng − *School of Petroleum Engineering, China University of Petroleum (East China), Qingdao 266580, China*

Complete contact information is available at:

https://pubs.acs.org/10.1021/acsomega.2c01550

Notes

The authors declare no competing financial interest.

■ ACKNOWLEDGMENTS

This work has been financially supported by the Dongying Science Development Fund (DJ2020001), the National Natural Science Foundation Project of China (51704311), the Changjiang Scholars and Innovative Research Team in University (IRT_14R58), the Fundamental Research Funds for the Central Universities (17CX02040A), the National Key Research and Development Program of China (2016YFC0304005), and the Project establishment and construction team of young and innovative talents introduction and education plan of colleges and universities in Shandong Province.

■ REFERENCES

(1) Wang, M.; Guang, X.; Kong, L. The prospects of applying shape memory polymer in petroleum engineering. *Pet. Drill. Tech.* **2018**, *46*, 14−20.

(2) Zhou, L.; Lu, Y.; Yi, X. Present situation of sand production prediction technology of oil wells in China. *Oil Gas Geol.* **2006**, *3*, 100−102.

(3) Wang, X.; Yang, W.; Yan, H.; Qin, C.; Shen, S. The sanding mechanism and sanding critical drawdown calculation in loose sandstone. *Nat. Gas Ind.* **2009**, *29*, 72−75.

(4) Dong, C.; Yan, Q.; Zhou, B.; Wang, Y.; Deng, J.; Song, J. Visual experimental simulation study on micro sand production form and sand production mechanism of weakly cemented reservoir. *Oil Drill. Prod. Technol.* **2020**, *42*, 227−235.

(5) Yu, F.; Jiang, Z.; Bai, J.; Liu, Y.; Meng, C. Determination of the temperature resistance capacity of sand control screen linear in horizontal heavy oil wells in the Bohai Oilfield. *Pet. Drill. Tech.* **2018**, *46*, 65−70.

(6) Cui, G.; Bao, C.; Jie, C.; Zhao, S.; Wei, Y.; Hao, Z.; Chai, L. Development of gravel pack sand control tool in open hole of horizontal well and its application in offshore oilfield. *Explor. Dev.* **2015**, *12*, 214−216.

(7) Dong, C.; Zhang, Q.; Gao, K.; Yang, K.; Feng, X.; Zhou, S. Optimization experiment and design model of sand retaining accuracy of mechanical screen pipe. *Pet. Explor. Dev.* **2016**, *43*, 991−996.

(8) Yan, C.; Li, Y.; Cheng, Y.; Wang, W.; Song, J.; Deng, F.; Feng, Y. Sand production evaluation during gas production from natural gas hydrates. *J. Nat. Gas Sci. Eng.* **2018**, *57*, 77−88.

(9) Han, Y.; Liu, P.; Lin, J.; Wang, X.; Jia, L. Application of cementing and gravel packing sand control integrated technology to sidetracked horizontal well: taking Caofeidian 11-2 Oilfield as an example. *Fault-Block Oil Gas Field* **2018**, *25*, 390−393.

(10) Hao, Z.; Zuo, K.; Liu, Y.; Li, N.; Wei, A.; Wang, M. Research andtesting of the integrated string for cementing and controlling sand in a medium-short radius wellbore. *Pet. Drill. Tech.* **2019**, *47*, 99−104.

(11) Wei, A.; Chen, S.; Xu, J.; Zuo, K.; Hao, Z.; Wang, M. Integrated cementing and sand control technology in offshore oilfields. *Oil Drill. Prod. Technol.* **2017**, *39*, 570−573.

(12) Wang, Y.; Li, C.; Lin, Y.; Yang, J. Research progress of application of SMA in petroleum engineering. *Mater. Rep.* **2016**, *30*, 98−102. 107

(13) Li, S.; Zhang, J.; Chen, J.; Liu, R.; Jiang, Z. Preparation and properties of shape memory polyurethane foam. *Polyurethane Ind.* **2019**, *34*, 20−22.

(14) Sun, D.; Chen, X.; Liang, W.; Jia, W.; Li, P. Preparation and performance evaluation of polyurethane-expandable material in sand control. *Oilfield Chem.* **2016**, *34*, 217−221.

(15) Fei, G.; Gong, Q.; Xia, H. Changes of electrical conductivity of shape memory polyurethane/carbon nanotube composites during shape memory and heat treatment. *Polym. Mater.: Sci. Eng.* **2021**, *37*, 6−15.

(16) Cui, H.; Wang, F.; Hu, J.; Tu, W. Research progress of shape memory polyurethane materials. *Mater. Rev.* **2017**, *31*, 1−6. 31

(17) Yuan, Y.; Goodson, J.; Johnson, M. H.; Gerrard, D. In-situ mechanical and functional behavior characterization of shape memory polymer for sand control applications. *SPE Drill. Completion* **2012**, *27*, 253−263.

(18) Ma, J.; Liu, Y.; Li, H.; Jin, X. Structural design and sand control mechanism of self-adaptive expansion sand control screen. *Oil Field Equip.* **2010**, *39*, 1−4.

(19) Ma, J.; Liu, Y.; Li, H.; Liu, Z. Experimental study on performance evaluation of adaptive expansion sand control screen. *Oil Field Equip.* **2011**, *40*, 5−9.

(20) Wang, Z.; Cui, K.; Jiang, G.; Hua, Z.; Xu, P.; Guo, Y.; Sun, H. Development and performance evaluation of temperature sensitive expandable plugging agent based on shape memory epoxy resin polymer. *Drill. Completion Fluid* **2020**, *37*, 412−420.

(21) Carpenter, C.; Chris, R. Advancement in Openhole Sand-Control Applications With Shape-Memory Polymer. *J. Pet. Technol.* **2017**, *69*, 102−104.

(22) Mansour, A.; Dahi Taleghani, A.; Salehi, S.; Li, G.; Ezeakacha, C. Smart lost circulation materials for productive zones. *J. Pet. Explor. Prod. Technol.* **2018**, *9*, 281−296.

(23) Metcalfe, P. Expandable sand screen technology increases production. *World Oil* **2000**, *221*, 94−95.

(24) Kevin, M. Using expandable sand screens in unconsolidated formations. *Offshore* **2000**, *1*, 52−53.

(25) Wang, M.; Guang, X.; Kong, L. Application prospect of shape memory polymers in petroleum engineering. *Pet. Drill. Tech.* **2018**, *46*, 14−20.

(26) Tong, Z.; Shen, Z.; Shi, B. Development of packer based on shape memory polymer. *Pet. Mach.* **2014**, *42*, 69−71.

(27) Yu, C.; Chen, Q.; Hou, X.; Shen, J. Study on chemically crosslinked shape memory polyurethane. *Mech. Sci. Tech.* **2001**, *20*, 69−70.

(28) Melekhin, A. O.; Isachenko, A. I.; Apyari, V. V.; Volkov, P. K.; Zolotov, Y. A. Effect of amines on formation of gold/polyurethane foam nanocomposites and its sensing opportunities. *Talanta* **2021**, *226*, 122−151.

(29) Fang, S.; Cheng, G.; Zhang, J.; Jiang, Z. Development of high density filled shape memory polyurethane foam. *New Chem. Mater.* **2017**, *13*, 238−240.

(30) Chang, J.; Xiao, H.; Xie, Z.; Bi, H.; Zheng, J.; Zhu, S.; Hou, J. Effects of different process parameters and interface modification on mode I Interlaminar Fracture Toughness of carbon fiber reinforced polyphenylene sulfide Composites. *Compos. Mater. Sci. Eng.* **2022**, *6*, 22−28.

(31) Zhang, M.; Gao, Y.; Zhang, Y.; Zhang, M.; Li, Z. Preparation and properties of polyphenylene sulfide/oxidized-polyphenylene sulfide composite membranes. *React. Funct. Polym.* **2021**, *160*, 104842.

(32) Duan, Y.; Liu, H.; Ai, S.; Qin, X.; Yue, H.; Liu, B. Expansion performance test of shape memory sieve tube. *Pet. Drill. Tech.* **2020**, *48*, 6−10.